

A decade of changing surface energy balance components over a large water region

Pakorn Petchprayoon^{*a}, Peter D. Blanken^b, Khalid Hussein^c,
Waleed Abdalati^c, Siam Lawavirotwong^a

^a Geo-Informatics and Space Technology Development Agency, Bangkok, Thailand; ^b Dept. of Geography, Univ. of Colorado-Boulder, Boulder, CO USA; ^c Cooperative Institute for Research in Environmental Sciences, Univ. of Colorado at Boulder, Boulder, CO USA

ABSTRACT

This study has investigated the physical processes of energy exchange between the water surface and atmosphere over Lake Huron. The four components of surface energy balance, including net radiation, latent heat, sensible heat, and heat storage, were estimated using the twelve years (2002-2012) daily MODIS data together with in-situ measurements. Good agreement was found between the seasonal turbulent heat fluxes calculated from satellite data and those from the direct measurements (eddy covariance method) with correlation coefficients of 0.94 and 0.95 for sensible heat and latent heat, respectively. There were temporal, spatial heterogeneities, and strong seasonal pattern for all of the four components, which were very high in summer and low in winter for net radiation and heat storage. In contrast, latent heat and sensible heat were very high in the winter and very low in the summer. Trend analysis revealed long term changes for each of the energy balance components, particularly the increase in latent heat which was equivalent to evaporation rate of 0.017 mm m^{-2} per year, indicating that lake evaporation increased by 2.0 mm m^{-2} over the twelve years observation period. This was possibly a result of a smaller amount of over lake ice cover and an increase in surface water temperature of Lake Huron.

Keywords: remote sensing, surface energy balance, lake

1. INTRODUCTION

Great Lakes are one of the highest intensively used freshwater systems on earth. The lakes contain approximately 23,000 km^3 of water, which correspond to roughly 20% of the world's surface freshwater^[1]. These interconnected freshwater lakes are shared between the United States and Canada and support many crucial uses^[2]. Recently, decreasing water levels have been experienced in the Great Lakes. This current phenomenon of water level variations is an important issue because it is constant with many climate change predictions, raising anxiety that the decreasing of Great Lakes water level possibly will continue^[3]. Lake Huron is one of the Great Lakes that has experienced a decrease in water levels. The lake is not controlled for hydroelectric power or business navigation and is simply minimally influenced by the inflow and outflow of the other lakes^[4]. Thus, the changes of water levels in Lake Huron are mainly reacting to climatic or other large-degree powers, including the physical control of the surface energy balance, which provides clues to how these drivers are changing.

One of the major components of the surface energy balance of large lakes and possibly the most complicated to calculate is evaporation from the lake surface^[5]. This term represents a major water loss and is an important factor in the lake's hydrology process^[6]. The eddy correlation technique for directly measuring the surface energy balance is considered to be the best approach for assessing evaporation^{[7][8]}. However, accurate measurements of the local energy balance components, particularly evaporation, are commonly completed only at a small number of research sites^[9]. There are few studies estimating the surface energy balance and evaporation over large lakes using highly-accurate direct measurements such as the eddy covariance method^{[10][11][12][13][14]}.

Regarding the energy balance approach, in comparison to the water budget approach, there are also few studies conducted on the Great Lakes. Bolsenga determined the evaporation over Lake Huron using the energy balance method^[15]. His results have shown reasonable agreement with the evaporation calculated with the mass transfer method. Lofgren and Zhu applied the lake surface temperature derived from satellite data together with meteorological data to calculate the surface energy fluxes on the Great Lakes^[16]. Blanken et al. conducted the first direct measurement of the surface energy balance using the eddy covariance method over Lake Superior from June, 2008 to present^[13]. Spence et al. applied remote sensing data together with a climate model to examine the spatial distribution of evaporation across all of Lake Superior from the summer of 2008 to the fall of 2010^[14]. However, the long-term (i.e. several years) estimates of evaporation and surface energy balance over Lake Huron using both techniques have not been reported. The major difficulty in estimating lake evaporation using the energy balance method is the lack of meteorological measurements on the lake and there is no adequate technique to interpolate the meteorological data from sparse surface observations. Regarding the eddy covariance systems, there are difficulties associated with the direct measurements of lake evaporation because they involve major financial investment in terms of devices, station maintenances, and field works^[17].

Long-term continuing observations and in-situ data are essential for understanding lake evaporation and evaluating the effects of evaporation change in water resources. The latent heat energy is one of the energy balance components that act as a connection between the energy and water budgets of the lake; thus changes in the energy of surface can make a significant change in water levels^[16]. Measuring the lake's energy balance is a very complicated and time-consuming procedure, because the factors that determine the energy intensity differ both spatially and temporally. Also, exchanges between the lake surface and atmosphere require updated information measured directly at the location. Since the surface area of the lake is so large, direct measurement of elements year-round over the entire water surface is not possible with currently-available resources.

Satellite remote sensing is most likely the only capable and practical technique to supply regional to global observations of some meteorological variables that are relevant to the calculation of surface energy balance, including net radiation, and latent and sensible heat fluxes. Regionally and globally-averaged quantities can be calculated without the under-sampling problem due to a limited number of observation networks^[18]. Therefore, application of specially-equipped remote sensing combined with spatially-constant surface meteorological parameters and GIS is necessary for assessing the magnitude of the surface energy balance of large lakes such as Lake Huron. It is also very useful for the research community to better understand the changes in the water level phenomenon that has been encountered in recent years.

The purpose of this chapter is to estimate the spatial and temporal variations, as well as the long-term changes in the Lake Huron's surface energy balance using MODerate resolution Imaging Spectroradiometer (MODIS) data, calibrated and verified by surface meteorological observations. The results of this study will be significant and beneficial in discovering the spatial and temporal distributions of the energy budget over large lakes. This will contribute to the research community studying climate both on regional and global scales. Furthermore, the results of this study will improve our understanding of the reasons behind the fluctuations in water levels.

This paper focuses on estimating the latent heat and sensible heat fluxes, but also presents details on the connections, between energy balance components and meteorological variables, seasonal changes of these components, and the water heat storage component. The first section describes the study area, followed by a description of the data and study methods. Next, the 2010 surface energy balance estimated from satellite data compared to direct measurements is presented. Next, a discussion of the seasonal spatial and temporal variations from the period 2002-2012 is given. Finally, conclusions are presented.

2. STUDY AREA

Lake Huron is the second largest surface fresh water of the Great Lakes, with the area of 59,600 km², and it is the third largest fresh water lake on earth. Lake Huron contains water volume of 3,540 km³, and a shoreline length (including islands) of 6,157 km^[19]. The lake has a length of 332 km and a greatest breadth of 245 km^[20]. Lake Huron is connected

to Lake Michigan, which lines at the similar surface elevation, by the narrow waterway Straits of Mackinac, assembly them geologically and hydrologically the single water body, which is known as Lake Michigan-Huron.

The Spectacle Reef Lighthouse, located 17.22 km east of the eastern end of Bois Blanc Island at 45.7732 N and 84.1367 W, is the only station measuring year-round meteorological variables over the lake. The station uses the eddy covariance method to measure the turbulent heat fluxes (both sensible and latent heat), net radiation, air temperature, humidity, rain rate, and lake surface temperature. The lighthouse is the major platform providing year-round, continuous 30-min average meteorological and fluxes data for estimating and validating the latent and sensible heat fluxes for this study.



Figure 1. Satellite mosaic images from MODerate Resolution Imaging Spectroradiometer (MODIS) showing the study area and location of Spectacle Reef Lighthouse with the meteorological station located on the top

3. OBJECTIVES

This study focuses on estimating the latent heat and sensible heat fluxes, but also presents heat storage and total heat fluxes into the lake surface by combining data from satellite and meteorological station data in order to discover the spatial and temporal distribution of the energy budget over Lake Huron. In order to achieve this goal, the objectives of this study are:

3.1 To examine the spatiotemporal variation of the latent heat and sensible heat fluxes as well as the surface energy balance using a combination of remotely-sensed data and field measurements

3.2 To determine the characteristic and long-term change of the surface energy balance component over a period of 11 years (2002-2012)

4. DATA AND METHODOLOGY

4.1 Data

Two kinds of datasets were used: satellite observation and direct surface-based measurements.

4.1.1 satellite data

Estimation of the latent heat flux, the sensible heat flux, and lake the surface energy balance were obtained throughout the period of 2002 –2012 at daily time intervals. Four data products from MODIS, including MOD03 (Geological product), MOD06 (Cloud product), MOD07 (Atmospheric profile product), and MOD11 (Land surface temperature product), were used. These data are in the Hierarchical Data Format-Earth Observing System (HDF-EOS), which contains multi-object files, and were obtained from the National Aeronautics and Space Administration MODIS Adaptive Processing System (MODAPS). The data are available at <http://modaps.nascom.nasa.gov/services/>. All products except MOD11 were extracted and mosaicked using the MODIS Conversion Toolkit (MCTK). For MOD11, the thermal images were extracted, reprojected, and mosaicked using the MODIS Reprojection Tool [21]. The nearest neighbour resampling was applied for all of the data in order to preserve the original pixel brightness [22]. The following are characteristic of each product.

The MOD03 product consists of geo-location field data calculated for each $1 \times 1 \text{ km}^2$ spatial resolution. The MOD03 contains latitude, longitude, surface height, solar zenith and azimuth angles, and satellite zenith and azimuth angles.

The MOD06 cloud product provides cloud information, including cloud optical thickness, cloud top temperature, cloud emissivity, and cloud fraction at spatial resolution of $5 \times 5 \text{ km}^2$.

The MODIS atmospheric profile product MOD07 provides air and dew point temperature profiles at a spatial resolution of $5 \times 5 \text{ km}^2$ at 20 levels of vertical atmospheric pressure.

MOD11 contains surface temperature at spatial resolutions of 1×1 and $5 \times 5 \text{ km}^2$, respectively for clear sky days.

4.1.2 In-situ Measurement

There are three sources of in-situ data: the meteorological station installed on top of the Spectacle Reef Lighthouse (45.773 N, 84.136 W), the NOAA National Data Buoy Center (station 45003 located at 45.351 N, 82.840 W), and the NOAA meteorological station on the Alpena Harbor Light (45.0560 N, 83.424 W). The Spectacle Reef Lighthouse is the major platform providing meteorological and fluxes data for calculating and validating the latent and sensible heat fluxes. The height of the instruments is 31 m above the mean water level, and the nearest shore is located 17.22km east of the eastern end of Bois Blanc Island. The latent heat and sensible heat were calculated using the method described by Blanken et al.^[13] over Lake Superior. The latent heat flux can be directly converted to mm of evaporated water by dividing by the latent heat of evaporation and the density of water. The vertical wind speed was measured using a 3-D sonic anemometer (model CSAT-3, Campbell Scientific, Logan, UT), whereas water vapour density was measured using a highly-sensitive hygrometer (model KH20, Campbell Scientific, Logan, UT). The statistics (means and covariances) of the high-frequency sampled data were collected at 30-min intervals using a datalogger (model CR23X, Campbell Scientific, Logan, UT). The DC power was supplied by four 12-V 115-Ah marine batteries charged by two 80-W solar panels. The datalogger and batteries were located in a dry location inside the lighthouse. Post-processing of these data, including quality control, was performed following Blanken et al.^[13].

4.2 Methodology

The general surface energy balance equation of a water body surface can be expressed by

$$Q^* = Q_E + Q_H + Q_S + Q_{GL} \quad (1)$$

where:

- Q^* is the net radiation (W m^{-2})
- Q_E is the latent heat flux (evaporative heat flux) (W m^{-2})
- Q_H is the sensible heat flux (W m^{-2})
- Q_S is heat storage in the water (W m^{-2})
- Q_{GL} is the heat conduction across the lake bottom (W m^{-2})

In large water bodies such as the Great Lakes, Q_{GL} is negligible because the heat loss through the lake bottom is presumably small compared to the surface radiative exchanges and the net advective components since solar radiation cannot penetrate to the lake bottom and all of the energy absorbed by the water volume^{[12][23]}. Also, the advection of heat from precipitation and the inflow and outflow in large, deep lakes are small compared to the radiation exchanges^[24]. The resulting surface energy balance for a large water body can therefore be simplified as:

$$Q^* = Q_E + Q_H + Q_S \quad (2)$$

4.2.1 Net Radiation

The equation for estimating net radiation can be expressed as:

$$Q^* = (1 - \alpha)K \downarrow + L \downarrow - L \uparrow \quad (3)$$

where

- α is the surface albedo (no units)
- $K \downarrow$ is the incoming shortwave radiation flux density ($W m^{-2}$)
- $L \downarrow$ is the incoming longwave radiation flux density ($W m^{-2}$)
- $L \uparrow$ is the outgoing longwave radiation flux density ($W m^{-2}$)

Surface Albedo, α

Fresnel reflection equation for un-polarized radiation^[25] was applied to estimate the reflectivity of the lake's surface. The equation can be written as:

$$\alpha(\theta, n) = \frac{1}{2} \left[\frac{\sin^2(\theta - n)}{\sin^2(\theta + n)} + \frac{\tan^2(\theta - n)}{\tan^2(\theta + n)} \right] \quad (4)$$

where:

- θ is solar zenith angle which was obtained from MOD03 Geological product
- n is the angle of refraction for the medium.

For water:

$$\sin n = \sin \frac{\theta}{m} \quad (5)$$

where:

- m is the index of refraction (1.33 for visible spectrum region)

Under cloudy sky conditions, values of albedo were calculated from field data collected over Great Slave Lake^[10]. We did not estimate albedo values directly from Lake Huron in-situ measurements, because the albedo signal was contaminated by the lighthouse's concrete base, which lead to overestimation of albedo values.

Incoming Shortwave Radiation, $K \downarrow$

Computation of incoming shortwave radiation for clear sky conditions was carried out using two parameters, vapor pressure and solar zenith angle. The method developed by Zillman cited in Bisht^[26] is used and the equation can be written as:

$$K \downarrow_{clear} = \frac{s_o \cos^2 \theta}{1.085 \cos(\theta) + e_o (2.7 + \cos(\theta)) \times 10^{-8} + \beta} \quad (6)$$

where :

- s_o is the solar constant 1376 Wm^{-2}
- β is a constant value 0.1
- e_o is vapor pressure (hPa)

Vapor pressure, e_o was calculated from dew point temperature data using Clausius-Clapeyron^[26] as the following equation:

$$e_o = 6.11 \exp \left[\frac{L_v}{R_v} \left(\frac{1}{273.15} - \frac{1}{T_d} \right) \right] \quad (7)$$

where :

- L_v is the latent heat of vaporization ($2.56 \times 10^6 \text{ Jkg}^{-1}$)
- R_v is the constant of gas for water vapor ($461 \text{ J kg}^{-1} \text{ K}^{-1}$)
- T_d is dew point temperature (K) derived from MOD07 atmospheric profile product

In case of cloudy sky conditions, we applied the method proposed by Slingo^[27], in which the incoming shortwave radiation (W m^{-2}) was calculated by weighting the shortwave radiation of clear sky using cloud fraction and cloud optical thickness. These two parameters were derived from MOD06 cloud product. The equation can be expressed as:

$$K \downarrow_{cloudy} = K \downarrow_{clear} \left[(1 - f_c) + f_c e^{-\tau_c / \cos(\theta)} \right] \quad (8)$$

where :

- f_c is cloud fraction (no units)
- τ_c is cloud optical thickness (no units)

Incoming Longwave Radiation, $L \downarrow$

Values for incoming longwave radiation (W m^{-2}) under clear-sky conditions were calculated using air temperature and air emissivity with the Stefan-Boltzman law.

$$L \downarrow = \sigma \epsilon_a T_a^4 \quad (9)$$

where :

- T_a is air temperature at the height of 31 m ($^{\circ}\text{K}$) from MOD07 atmospheric profile product
- σ is Stefan-Boltzman constant $5.67 \times 10^{-8} \text{ Wm}^{-2}\text{K}^{-4}$

ε_a is effective air emissivity (no units)

Effective air emissivity was estimated by Prata approach^[28]:

$$\varepsilon_a = 1 - (1 + \mathcal{G}) \exp\left(\sqrt{1.2 + 3\mathcal{G}}\right), \text{ with } \mathcal{G} = \left(\frac{46.5}{T_a}\right) e_o \quad (10)$$

In the case of cloudy conditions, some pixels values of MOD07 were missing (between 40 – 85 % missing value during summer and winter season). Thus, MODIS's surface temperature from MOD06 cloud product was employed to fill in these missing values of dew point temperature and air temperature by calculating temperature offsets. These offsets were computed as the difference between the MOD06 surface temperatures and the *in-situ* data from the Spectacle Reef meteorological station. The difference between surface water temperature and air temperature (dew point temperature) also was not constant year around. The offset was varied with season, particularly during winter, due to the difference in heat capacity between air and water. Thus, this study proposed calculating separate temperature offsets for winter and non-winter season. Then, incoming long-wave radiation during all sky conditions was estimated as a combination of incoming long-wave during clear sky condition and long-wave emitted from clouds.

$$L \downarrow = \varepsilon_a T_a^4 + \sigma((1 - \varepsilon_a) \varepsilon_c T_c^4) \quad (11)$$

where :

T_c is cloud temperature (K)

ε_c is cloud emissivity

Both cloud temperature and cloud emissivity was obtained from MOD06 cloud product.

Outgoing Long-wave Radiation $L \uparrow$

Outgoing long-wave radiation was calculated using MODIS's thermal surface temperature for all sky conditions. Under cloudy sky, MODIS's cloud free data composite image (MOD11A2, 8 days composite product) was employed to fill in these missing value pixels. However, it was found that during the winter season, there were some areas where new temperature imagery may not be available for more than 10 days because of cloud cover^[29]. To overcome this problem of missing data in both MOD11A1 and MOD11A2, spatial Inverse Distance Weighted (IDW) interpolation technique was used to calculate the missing pixels values of MOD11A2. Then the values of MOD11A2 were used to fill the missing values in daily MODIS data (MOD11A1). However, using MOD11A2 to fill the missing data pixels in MOD11A1 could introduce uncertainty because, the composite MOD11A2 data may be collected at different view angles, on different dates, and under different atmospheric conditions. Thus, it is necessary to validate the data before using them. The emitted long-wave radiation was calculated using the Stefan-Boltzman relationship, which can be written as:

$$L \uparrow = \varepsilon_s T_s^4 \quad (12)$$

where :

T_s is water surface temperature (K)

ε_s is emissivity of water surface

4.2.2 Latent heat flux

The evaporative (latent) Q_E heat flux term from the remote sensing estimates of lake-wide conditions was calculated using the bulk aerodynamic formulae. The latent heat flux was calculated as follows^[30]:

$$Q_E = \rho_A L_V c_E |U| [e_{SAT}(T_S) - r e_{SAT}(T_A)] \frac{0.622}{p_A} \quad (13)$$

where:

- ρ_A is the air density (1.2 kg m^{-3})
- L_V is the vaporization of latent heat ($2.501 \times 10^6 \text{ J kg}^{-1}$)
- c_E is a coefficient of turbulent exchange (no units)
- U is the horizontal wind speed (m s^{-1})
- e_{SAT} is the saturation vapour pressure (hPa)
- T_S is the water surface temperature ($^{\circ}\text{C}$)
- r is the relative humidity (no units)
- T_A is the air temperature ($^{\circ}\text{C}$)
- p_A is the atmospheric surface pressure (hPa)

Relative humidity r can be calculated using the equation:

$$r = \frac{e}{e_{SAT}} \times 100 \quad (14)$$

where:

- e is the ambient vapour pressure (hPa)

Saturation vapour pressure e_{SAT} was calculated using the Magnus-type equations^[31].

$$e_{SAT} = 6.1094 \exp\left(\frac{17.625T}{243.04 + T}\right) \quad (15)$$

Complete long term in-situ measurements of wind speed, even from a single station, were not available. Thus, some constraints were imposed on the wind speed (U) and coefficient of turbulent exchange for the water vapour (c_E). Wind speed data were collected from three different meteorological station sites: Spectacle Reef Lighthouse (main station), NOAA's National Data Buoy Center (station 45003), and NOAA's meteorological station on the Alpena Harbor Light, because no single meteorological station was available for the entire study period. The wind field was considered homogeneous for the whole lake, since there were no multiple meteorological stations covering the entire lake. Therefore, this study used wind speed at the height of 12 m (before October 27, 2005) and at of 18 m (after October 27, 2005) because the wind speed sensor was moved to a higher position. Since all of the parameters and results from this study were compared to the in-situ based measurements at the height the observations at Spectacle Reef lighthouse (31 m), the wind speed was extrapolated at the NOAA station's measured height (12 m and 18 m) to a height of 31 m (Spectacle Reef Lighthouse) using the standard power law equation^[24]. The increase of wind speed with height can be calculated by:

$$U_2 = U_1 \times \left(\frac{Z_2}{Z_1} \right)^{1/7} \quad (16)$$

where:

- U_1 is known horizontal wind velocity at level Z_1 (m s^{-1})
- U_2 is the wind velocity to be calculated at height level Z_2 (m s^{-1})
- Z_1 reference height where U_1 is known (m)
- Z_2 is the height above lake level for velocity U_2 (m)

Due to a lack of spatial data representation over the Great Lakes, the above equation was applied without adjusting for stability^[24] since there were no direct measurements of the sensible heat flux and friction velocity during the time before September 2009 that were required to calculate the atmospheric stability using either the Richardson Number or Monin-Obukov Length. Thus, the stability condition over the lake could not be estimated and adjustment of wind speed at different height was done without reference to a stability correction.

After the wind speed was extrapolated to the height of the Spectacle Reef Lighthouse station, regression analysis was applied to determine the relationship between the wind speed measured at the lighthouse station and each of the other two stations for four seasons.

The coefficients of the turbulent exchange of the latent heat flux (c_E) were also considered to have similar spatial value for the whole lake. Alcantara *et al.* [32] assumed that c_E had a constant value of 1.1×10^{-3} for both temporal and spatial coverage in the study of heat fluxes over the Itumbiara Reservoir in Brazil. Also, Derecki^[6] and Quinn^[33] assumed that the c_E and c_H were equal for a study of Great Lakes evaporation. This study proposed to calculate the coefficients of turbulent exchange c_E and c_H for Lake Huron using latent heat, wind speed, surface temperature, air temperature, and vapour pressure gradient data observed from the meteorological station at the Spectacle Reef Lighthouse from 2010-2011. The coefficient of turbulent exchange for the latent heat was estimated as (adjusted from Alcantara *et al.*^[32]):

$$c_E = \frac{Q_E P_A}{6.22 \times \rho_A L_V |U| [e_{SAT}(T_S) - r e_{SAT}(T_A)]} \quad (17)$$

4.2.3 Sensible heat flux

The sensible Q_H heat flux term was estimated using equation^[30]

$$Q_H = \rho_A c_p c_H |U| (T_S - T_A) \quad (18)$$

where:

- c_p is the specific heat capacity of air ($1.005 \times 10^3 \text{ kg m}^{-3}$)
- c_H is a coefficient of turbulent exchange (no units)

The same assumptions used for estimation of c_E were applied for the calculation of the coefficient of turbulent exchange for sensible heat (c_H). The c_H was estimated using the following equation: (adjusted from Alcantara *et al.*^[32])

$$c_H = \frac{Q_H}{\rho_A c_p |U| (T_S - T_A)} \quad (19)$$

The odd values of C_E and C_H were removed using the standard deviation (sigma) specific to each year. The coefficient values greater than the value of two sigma above the mean value and lower than the value of two sigma below the mean value were eliminated.

4.2.4 Heat Storage

The heat storage term was estimated as a residual of the surface energy balance:

$$Q_S = Q^* - Q_E - Q_H \quad (19)$$

4.3 Comparison of latent heat and sensible heat to the ground-based observations

For the comparison, latent and sensible heat fluxes calculated for 2010 and 2011 were used. The latent heat and sensible heat fluxes calculated from satellite parameters, together with wind speed data and the coefficients of turbulent exchange from meteorological stations, were compared to the heat fluxes derived using the eddy correlation method, which is a direct measurement technique.

4.4 Spatial and temporal variations in lake surface energy balance

Maps of the daily surface energy balance components of Lake Huron were created with a $5 \times 5 \text{ km}^2$ grid resolution in order to examine the temporal and spatial distribution of the surface energy balance components in different seasons. All of the remote sensing estimates of lake-wide conditions were calculated using ERDAS IMAGINE 9.2 and ArcMap version 10.1 using the Python programming language.

To calculate the change of surface energy balance components, least squares linear regression was applied for each pixel with daily temporal resolution over 11 years. The slope of each regression line represents the net radiation change during the study period.

5. RESULTS AND DISCUSSION

5.1 View the pre-formatted styles

Figure 3 shows the seasonal surface energy balance components for the study period. The seasonal latent heat estimated from the satellite for the period of 2010-2011 was very close to the estimates of the eddy correlation method ($R^2 = 0.95$). The maximum net radiation was received during the summer when it reached a value greater than 700 W m^{-2} and the minimum was in the winter ($\sim 200 \text{ W m}^{-2}$). Almost all of the net radiation was stored as heat in the lake. In the fall, the net radiation began to decrease and the lake started to release the stored energy into the atmosphere through sensible and latent heat fluxes by releasing all of the stored heat. The latent and sensible heat fluxes reached their maximum in the winter. The spatial ice cover data were not accounted for in the estimation of the heat fluxes and thus the results of the turbulent heat fluxes presented in this study during the winter season might have been overestimated, particularly during exceptionally cold years (2003 and 2009). This is because the turbulent heat fluxes could have been greatly reduced by the formation of ice^[13].

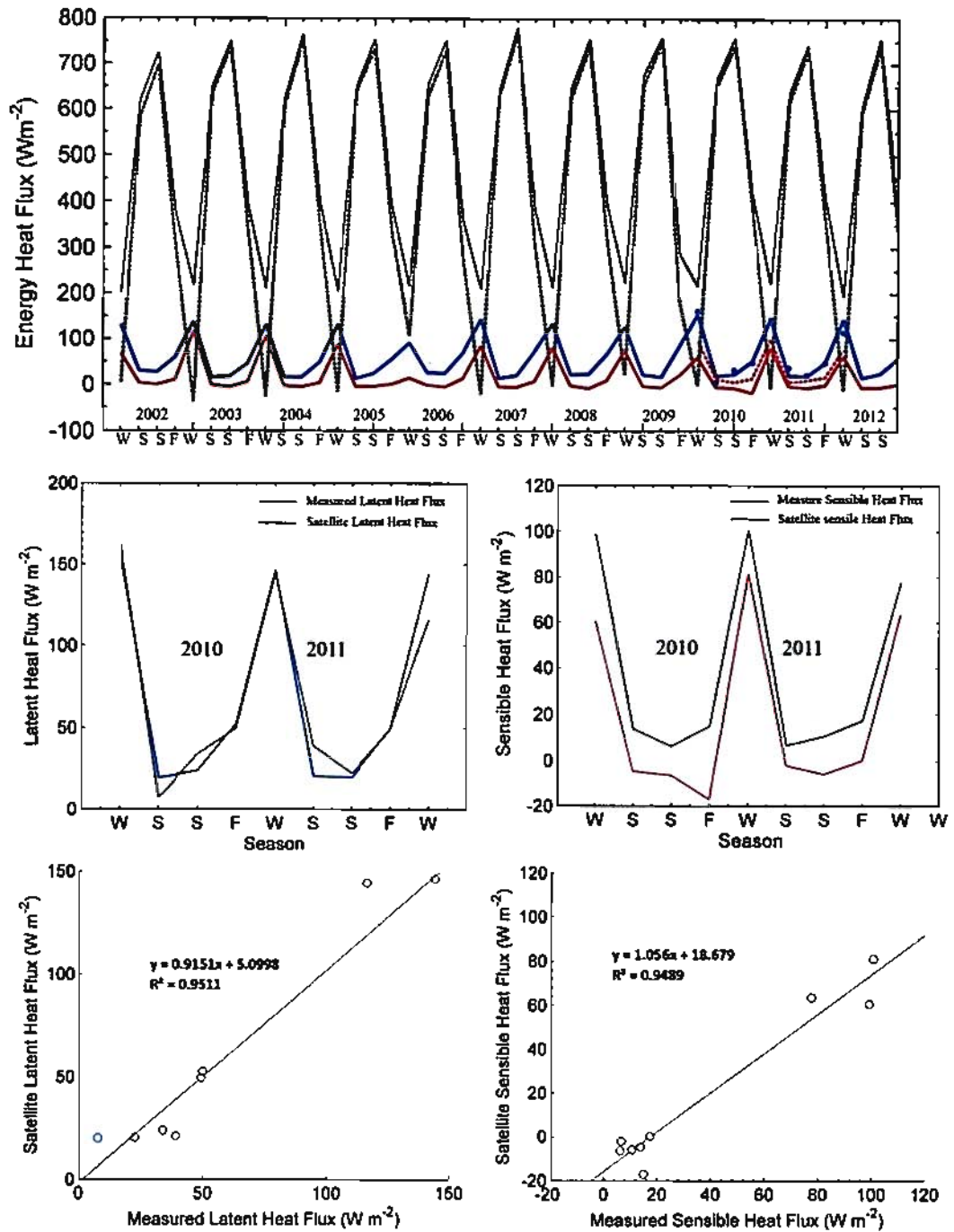


Figure 2. (Top Panel) Seasonal surface energy balance components for the period 2002-2012. Net radiation is the grey dotted line, the gray color is heat storage, and the blue and red represent latent and sensible heat fluxes, respectively. The blue and red dotted line (year 2010-2011) show the latent (blue) and sensible (red) heat derived using the eddy covariance method. The middle and lower panel present a comparison and scatterplot of the seasonal satellite turbulent heat fluxes derived using the eddy covariance method.

To see the formats available with this manuscript, go to the Format menu and choose "Styles and Formatting". To view which style is being used in any part of this document, place your cursor on the line and look in the Styles and Formatting display.

5.2 Energy balance components and their spatial distribution

The mean seasonal instantaneous surface energy balance components with spatial standard deviation values are presented in Table 1. Net radiation and heat storage reached their highest values in the summer season (months JJA) and the lowest values were in the winter season (months DJF). In contrast, the latent and sensible heat fluxes reached their seasonal maximum in the winter periods and their minimum intensity during the spring and summer periods.

Table 1. Seasonal mean heat fluxes ($W m^{-2}$) average over Lake Huron, with spatial standard deviation in parentheses. The value was based on the heat fluxes of 2002 to 2004 and 2012

Season	Latent heat flux	Sensible heat flux	Net radiative flux	Heat storage
Winter (DJF)	84.04 (27.27)	14.94 (33.18)	224.57 (14.69)	125.59 (67.44)
Spring (MAM)	29.49 (36.01)	0.28 (3.35)	620.80 (14.78)	591.03 (30.82)
Summer (JJA)	26.15 (11.69)	-2.45 (4.25)	755.56 (13.27)	731.86 (27.12)
Fall (MAM)	59.82 (7.73)	3.52 (3.72)	394.46 (13.47)	331.11 (19.15)

The spatial distributions of the average seasonal surface energy balance components, including net radiation, latent heat flux, sensible heat flux, and the heat storage term for Lake Huron obtained from the remote sensing satellite and meteorological data between 2002 to 2004 and 2012, were produced. The color (and gray scale) schemes illustrated seasonal mean instantaneous (i.e. during the satellite overpass) radiation and heat flux values, and the dark (cold tone color) areas represented the lower values of heat fluxes and radiation, while the bright (warm tone color) areas meant higher intensities of heat fluxes and radiation fluxes. The following are details of the spatial distribution for each surface energy balance component.

5.2.1. Net radiation

Daily instantaneous net radiation calculated from the previous chapter was reproduced to a seasonal average as shown in Figure 3(a) and Figure 4(a). The net radiation was mainly controlled by incident solar radiation, adjusted by cloud cover, and surface albedo. It was also influenced by the incoming long-wave radiation as a function of air temperature, vapour pressure, and cloud cover, and by outgoing long-wave radiation, depending on the lake surface water temperature.

In the winter (DJF), the spatial distribution of the net radiation had an approximately regular latitudinal pattern, which was primarily controlled by the solar zenith angle. The winter presented the lowest mean radiation value of $224.57 W m^{-2}$. During spring (MAM), with the increase of solar elevation, the net radiation increased to almost three times the mean winter value, but the latitudinal character was not obvious.

In the summer (JJA), the spatial distribution of net radiation over the lake did not show a latitudinal trend. The variability of net radiation was related to the lake's surface temperature and the presence or absence of cloud cover. In the fall (SON), the net radiation decreased and it was almost two times less than the mean net radiation for the summer. This was primarily due to the decrease in solar elevation.

5.2.2 Latent heat flux

The transfer of latent heat from the lake surface was mainly controlled by wind speed, water temperature, air temperature, and amount of vapour pressure. There were large latent heat fluxes in the wintertime and much smaller values in spring and summer. The seasonal mean spatial variability of the latent heat fluxes is presented in Figure 3(b) and Figure 4(b). The winter period exhibited the greatest latent heat flux over the lake-wide area, particularly in the